

Theoretical studies of a three-band Hubbard model with a strong spin-orbit coupling for 5d transition metal oxide Sr_2IrO_4

Tomonori Shirakawa^{1,2,3}, Hiroshi Watanabe^{1,2,3} and Seiji Yunoki^{1,2,3}

¹Computational Materials Science Research Team, RIKEN AICS, Kobe, Hyogo 650-0047, Japan

²Computational Condensed Matter Physics Laboratory, RIKEN ASI, Saitama 351-0198, Japan

³CREST, Japan Science and Technology (JST), Kawaguchi, Saitama 332-0012, Japan

E-mail: t-shirakawa@riken.jp

Abstract. Motivated by recent experiments on Sr_2IrO_4 , we study the ground state properties of a two-dimensional three-band Hubbard model with a strong relativistic spin-orbit coupling. Using the exact diagonalization technique, the dynamical magnetic structure factor $M(\mathbf{q}, \omega)$ is calculated to examine the low-energy magnetic excitations. We find that the low-energy excitations in $M(\mathbf{q}, \omega)$ are well described by an effective Heisenberg model composed of a local Kramers doublet of an effective total angular momentum $J_{\text{eff}} = |\vec{s} - \vec{\ell}| = 1/2$. The antiferromagnetic exchange interaction estimated from $M(\mathbf{q}, \omega)$ is as large as ~ 80 meV, which is in good quantitative agreement with experiments. To study a possible long-range ordered state in the thermodynamic limit, we use the variational cluster approximation based on the self-energy functional theory, which is parallelized to accelerate the calculations. We find the ground state where the local Kramers doublet is in-plane antiferromagnetically ordered.

1. Introduction

5d transition metal oxides in a layered perovskite structure such as Sr_2IrO_4 [1] and Ba_2IrO_4 [2] have attracted much attention because of their unique properties caused by a strong relativistic spin-orbit coupling (SOC) of 5d transition element. It has been observed experimentally that these materials behave like an effective total angular momentum $J_{\text{eff}} = |\vec{s} - \vec{\ell}| = 1/2$ Mott insulator at low temperatures [2, 3, 4], where \vec{s} ($\vec{\ell}$) is the spin (orbital) angular momentum operator. Moreover, very recent experiments using muon spin rotation (μSR), magnetic susceptibility, and resonant inelastic x-ray scattering (RIXS) have revealed that the low-energy magnetic excitations can be described by an “isospin”-1/2 Heisenberg model with an effective exchange interaction as large as ~ 60 -100 meV [2, 5, 6], which is almost comparable to the ones in the parent compounds of high- T_c cuprate superconductors [7].

Motivated by these experiments, we study theoretically the nature of magnetic excitations for Sr_2IrO_4 using a three-band Hubbard model with the SOC. For this purpose, here the numerically exact diagonalization technique is employed. We find that the low-energy magnetic excitations are described by an antiferromagnetic Heisenberg model with the nearest-neighbor exchange coupling as large as ~ 80 meV. Furthermore, to study the stability of this antiferromagnetically ordered state, we use the variational cluster approximation (VCA) [8] based on the self-energy



functional theory (SFT) [9]. The VCA is efficiently parallelized up to ~ 300 cores. We find that the ground state is in-plane antiferromagnetically ordered with the $J_{\text{eff}} = 1/2$ local Kramers doublet. This finding is in good agreement with experiments [3, 4, 5].

This paper is organized as follows. In Section 2, we introduce an effective three-band Hubbard model for Sr_2IrO_4 . The magnetic excitations of this model are next discussed in Section 3. After giving brief explanation of VCA and description of its parallelization scheme, the stability of an antiferromagnetically ordered state is discussed in Section 4. Finally, Section 5 concludes this paper.

2. Model

The local electronic configuration of Ir^{4+} ion in Sr_2IrO_4 is a low-spin state with $(t_{2g})^5$ because of the large crystalline field effect, which is estimated much larger than the SOC and the local Coulomb interactions [10]. Thus, one of the simplest models which capture the low-energy physics of Sr_2IrO_4 is the following effective Hubbard model, consisting of three t_{2g} orbitals (d_{xy} , d_{yz} , and d_{zx}), defined on a square lattice [11],

$$H = H_{\text{kin}} + H_{\text{so}} + H_U, \quad (1)$$

where

$$H_{\text{kin}} = \sum_{\mathbf{k}} \sum_{\alpha, \sigma} \varepsilon_{\mathbf{k}}^{\alpha} c_{\mathbf{k}, \alpha, \sigma}^{\dagger} c_{\mathbf{k}, \alpha, \sigma}, \quad (2)$$

$$H_{\text{so}} = \lambda \sum_{\mathbf{r}} \sum_{\alpha, \beta} \sum_{\sigma, \sigma'} \langle \phi_{\mathbf{r}\alpha\sigma} | \vec{\ell} \cdot \vec{s} | \phi_{\mathbf{r}\beta\sigma'} \rangle c_{\mathbf{r}, \alpha, \sigma}^{\dagger} c_{\mathbf{r}, \beta, \sigma'}, \quad (3)$$

$$H_U = U \sum_{\mathbf{r}\alpha} n_{\mathbf{r}, \alpha, \uparrow} n_{\mathbf{r}, \alpha, \downarrow} + \frac{1}{2} (U' - J) \sum_{\mathbf{r}\sigma} \sum_{\alpha \neq \beta} n_{\mathbf{r}, \alpha, \sigma} n_{\mathbf{r}, \beta, \sigma} + \frac{U'}{2} \sum_{\mathbf{r}\sigma} \sum_{\alpha \neq \beta} n_{\mathbf{r}, \alpha, \sigma} n_{\mathbf{r}, \beta, \bar{\sigma}} - J \sum_{\mathbf{r}} \sum_{\alpha \neq \beta} c_{\mathbf{r}, \alpha, \uparrow}^{\dagger} c_{\mathbf{r}, \alpha, \downarrow} c_{\mathbf{r}, \beta, \downarrow}^{\dagger} c_{\mathbf{r}, \beta, \uparrow} + J' \sum_{\mathbf{r}} \sum_{\alpha \neq \beta} c_{\mathbf{r}, \alpha, \uparrow}^{\dagger} c_{\mathbf{r}, \alpha, \downarrow}^{\dagger} c_{\mathbf{r}, \beta, \downarrow} c_{\mathbf{r}, \beta, \uparrow}. \quad (4)$$

Here, $c_{\mathbf{r}, \alpha, \sigma}^{\dagger}$ ($c_{\mathbf{r}, \alpha, \sigma}$) represents the creation (annihilation) operator of an electron with spin $\sigma = (\uparrow, \downarrow)$ and orbital $\alpha = (xy, yz, zx)$ on site \mathbf{r} , $n_{\mathbf{r}, \alpha, \sigma} = c_{\mathbf{r}, \alpha, \sigma}^{\dagger} c_{\mathbf{r}, \alpha, \sigma}$, $c_{\mathbf{k}, \alpha, \sigma}^{\dagger}$ is the Fourier transform of $c_{\mathbf{r}, \alpha, \sigma}^{\dagger}$, and $\bar{\sigma}$ indicates the opposite spin of σ . The number N_e (N_h) of electrons (holes) is set to be $5N$ (N), where N is the number of sites. $\varepsilon_{\mathbf{k}}^{\alpha}$ is the energy dispersion of orbital α defined by

$$\varepsilon_{\mathbf{k}}^{xy} = -2t_1(\cos k_x + \cos k_y) - 4t_2 \cos k_x \cos k_y - 2t_3(\cos 2k_x + \cos 2k_y) + \Delta, \quad (5)$$

$$\varepsilon_{\mathbf{k}}^{yz} = -2t_4 \cos k_y - 2t_5 \cos k_x, \quad (6)$$

$$\varepsilon_{\mathbf{k}}^{zx} = -2t_4 \cos k_x - 2t_5 \cos k_y, \quad (7)$$

where Δ is the energy level difference between d_{xy} and the others [10, 11]. The relativistic SOC term is described by H_{so} in (3), where $\phi_{\mathbf{r}\alpha\sigma}$ is the Wannier orbital with spin σ and orbital α at site \mathbf{r} . We assume the matrix elements $\langle \phi_{\mathbf{r}\alpha\sigma} | \vec{\ell} \cdot \vec{s} | \phi_{\mathbf{r}'\beta\sigma'} \rangle$ are finite only for $\mathbf{r} = \mathbf{r}'$. H_{so} is then written in the matrix form

$$H_{\text{so}} = \frac{\lambda}{2} \sum_{\mathbf{r}\sigma} \left(c_{\mathbf{r}, xy, \bar{\sigma}}^{\dagger}, c_{\mathbf{r}, yz, \sigma}^{\dagger}, c_{\mathbf{r}, zx, \sigma}^{\dagger} \right) \begin{pmatrix} 0 & -s_{\sigma} & -i \\ -s_{\sigma} & 0 & is_{\sigma} \\ i & -is_{\sigma} & 0 \end{pmatrix} \begin{pmatrix} c_{\mathbf{r}, xy, \bar{\sigma}} \\ c_{\mathbf{r}, yz, \sigma} \\ c_{\mathbf{r}, zx, \sigma} \end{pmatrix}, \quad (8)$$

where $s_{\uparrow} = +1$ ($s_{\downarrow} = -1$). Equation (4) describes the Coulomb interaction term which includes intra-orbital Coulomb repulsion U , inter-orbital Coulomb repulsion U' , Hund's coupling J , and pair hopping term J' with $U = U' + 2J$ and $J = J'$ [12].

A set of parameters $\mathbf{t} = (t_1, t_2, t_3, t_4, t_5, \Delta, \lambda) = (0.36, 0.18, 0.09, 0.37, 0.06, -0.36, 0.37)$ eV in $H_{\mathbf{t}} = H_{\text{kin}} + H_{\text{so}}$ for Sr_2IrO_4 [11] is determined to reproduce the energy band dispersion calculated by the first-principles electronic structure calculations based on the density functional theory [10]. In this paper, we set $U/t_1 = 6.111$ and $J/U = 0.1$. These values are similar to the ones estimated by the constrained random phase approximation [13, 14].

3. Exact diagonalization study on magnetic excitations

In this section, the magnetic excitations are studied using the numerically exact diagonalization technique. Because of the exponential increase of the Hilbert space with N , the system sizes that can be treated are limited. However, this method provides the unbiased results, which are valuable and complementary to other approximate calculations such as VCA.

3.1. Method

We employ the numerically exact diagonalization technique for a cluster of $\sqrt{8} \times \sqrt{8}$ with periodic boundary conditions. To reduce the Hilbert space dimensions, we fully use the symmetry of Hamiltonian, i.e., translational symmetry and spin inversion symmetry. We first use the Lanczos algorithm [15] to calculate the ground state $|\psi_0\rangle$ and the ground state energy E_0 . Then, the continued fraction expansion [15] is used to calculate the dynamical correlation function for an operator \mathcal{O} , which is defined by

$$C_{\mathcal{O}}(\omega) = -\frac{1}{\pi} \text{Im} \langle \psi_0 | \mathcal{O}^\dagger (\omega + i\eta - H + E_0)^{-1} \mathcal{O} | \psi_0 \rangle, \quad (9)$$

where $\eta(>0)$ is a broadening factor. Note that the static correlation function $S_{\mathcal{O}} = \langle \psi_0 | \mathcal{O}^\dagger \mathcal{O} | \psi_0 \rangle$ is related to the dynamical correlation function by $S_{\mathcal{O}} = \int d\omega C_{\mathcal{O}}(\omega)$. Following the notation in (9), the dynamical magnetic structure factor is given by $M_{\xi}(\mathbf{q}, \omega) = C_{\mathcal{O}}(\omega)$ with $\mathcal{O} = M_{\xi}(\mathbf{q}) = 2S_{\xi}(\mathbf{q}) + L_{\xi}(\mathbf{q})$, where $S_{\xi}(\mathbf{q})$ [$L_{\xi}(\mathbf{q})$] is the Fourier transform of the ξ ($= x, y, z$) component of the local spin (orbital) angular momentum operator $S_{\mathbf{r}}^{\xi}$ ($L_{\mathbf{r}}^{\xi}$),

$$S_{\mathbf{r}}^{\xi} = \frac{1}{2} \sum_{\alpha} \sum_{\sigma_1 \sigma_2} c_{\mathbf{r}, \alpha, \sigma_1}^{\dagger} (\hat{\sigma}_{\xi})_{\sigma_1, \sigma_2} c_{\mathbf{r}, \alpha, \sigma_2}, \quad (10)$$

$$L_{\mathbf{r}}^{\xi} = \begin{cases} i \sum_{\sigma} (c_{\mathbf{r}, zx, \sigma}^{\dagger} c_{\mathbf{r}, xy, \sigma} - c_{\mathbf{r}, xy, \sigma}^{\dagger} c_{\mathbf{r}, zx, \sigma}) & (\xi = x) \\ i \sum_{\sigma} (c_{\mathbf{r}, xy, \sigma}^{\dagger} c_{\mathbf{r}, yz, \sigma} - c_{\mathbf{r}, yz, \sigma}^{\dagger} c_{\mathbf{r}, xy, \sigma}) & (\xi = y) \\ i \sum_{\sigma} (c_{\mathbf{r}, yz, \sigma}^{\dagger} c_{\mathbf{r}, zx, \sigma} - c_{\mathbf{r}, zx, \sigma}^{\dagger} c_{\mathbf{r}, yz, \sigma}) & (\xi = z) \end{cases}, \quad (11)$$

and $\hat{\sigma}_{\xi}$ is the ξ component of the Pauli matrix.

3.2. Results

The results for the dynamical magnetic structure factor $M_{\xi}(\mathbf{q}, \omega)$ for Sr_2IrO_4 are shown in the left panels of figure 1. Although there are several peaks in each momentum \mathbf{q} , we will show below that the low-energy spectral peaks below $\sim 0.5t_1$ are identified as the magnetic excitations of the local Kramers doublet.

Let us first define a quasi-particle operator by

$$a_{\mathbf{r}, \theta, \sigma}^{\dagger} = s_{\sigma} \cos \theta c_{\mathbf{r}, xy, \sigma}^{\dagger} + \frac{\sin \theta}{\sqrt{2}} (c_{\mathbf{r}, yz, \bar{\sigma}}^{\dagger} + i s_{\sigma} c_{\mathbf{r}, zx, \bar{\sigma}}^{\dagger}), \quad (12)$$

characterizing a slightly generalized $J_{\text{eff}} = 1/2$ -like local Kramers doublet [16, 17]. The value of θ is determined by maximizing the hole density $n_{\theta, \sigma} = \langle \psi_0 | a_{\mathbf{r}, \theta, \sigma} a_{\mathbf{r}, \theta, \sigma}^{\dagger} | \psi_0 \rangle$. Next, using this

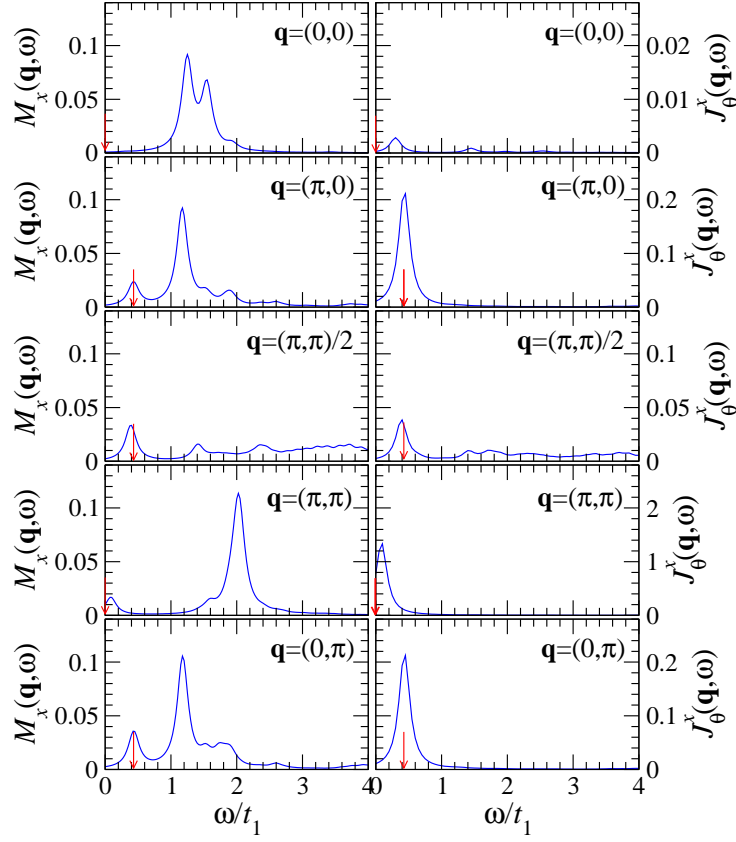


Figure 1. Dynamical magnetic structure factor $M_x(\mathbf{q}, \omega)$ (left panels) and dynamical correlation function $J_\theta^x(\mathbf{q}, \omega)$ (right panels) (see the text for definition) for several momenta \mathbf{q} indicated in the figures. A set of parameter used is for Sr_2IrO_4 mentioned in text. The broadening factor η used here is $\eta = 0.1t_1$. Red arrows indicate the position of the magnon dispersion of an isotropic “isospin”-1/2 Heisenberg model with the nearest neighbor exchange interaction $0.22t_1$ ($= 79$ meV).

quasi-particle operator, we construct a pseudo-spin operator $J_\theta^\xi(\mathbf{r})$:

$$J_\theta^\xi(\mathbf{r}) = \frac{1}{2} \sum_{\sigma_1, \sigma_2} a_{\mathbf{r}, \theta, \sigma_1}^\dagger (\hat{\sigma}_\xi)_{\sigma_1, \sigma_2} a_{\mathbf{r}, \theta, \sigma_2}. \quad (13)$$

Then, we calculate the dynamical correlation function for $J_\theta^\xi(\mathbf{q})$, i.e., $J_\theta^\xi(\mathbf{q}, \omega) = C_\mathcal{O}(\mathbf{q}, \omega)$ with $\mathcal{O} = J_\theta^\xi(\mathbf{q})$, where $J_\theta^\xi(\mathbf{q})$ is the Fourier transform of $J_\theta^\xi(\mathbf{r})$. The results for $J_\theta^x(\mathbf{q}, \omega)$ are shown in the right panels of figure 1. Comparing these two spectra $M_x(\mathbf{q}, \omega)$ and $J_\theta^x(\mathbf{q}, \omega)$ in figure 1, we find that the position of the low-lying peak at each \mathbf{q} in $M_x(\mathbf{q}, \omega)$ are exactly the same as the one in $J_\theta^x(\mathbf{q}, \omega)$ [18]. This is the direct numerical evidence that the low-energy magnetic excitations correspond nicely to the excitations of the local Kramers doublet.

Assuming that the low-energy excitation dispersions are expressed by the magnon dispersion $\omega_{\mathbf{k}}$ of an isotropic “isospin”-1/2 Heisenberg model, i.e., $\omega_{\mathbf{k}} = 2J\sqrt{1 - (\cos k_x + \cos k_y)^2/4}$, we can estimate an effective exchange interaction J . As shown in figure 1, we find that J is as large as $\sim 0.22t_1$ ($= 79$ meV). This value is in good agreement with experimental observations [2, 6, 5].

4. Variational Cluster Approximation (VCA) study on the long-range ordered ground state

In the previous section, we have found that the low-energy magnetic excitation is well described by the effective antiferromagnetic Heisenberg model composed of the local Kramers doublet. However, the method used in Section 3 is not suitable to study properties in the thermodynamic limit. To access the thermodynamic limit and study a possible long-range ordered state, here we employ an approximation technique called VCA.

4.1. Method

The VCA [8] based on the SFT [9] is one of cluster approaches to study interacting fermion systems on lattices. In this method, we first divide the original system into small clusters, such that each of them can be treated by the exact diagonalization technique. This set of small clusters is called a “reference system” below. In order to apply the VCA, the interacting part in the reference system must be the same as that in the original system, which is certainly satisfied in (1). However, the non-interacting part such as the kinetic energy term and the SOC term can be different. Here, we shall denote by \mathbf{t}' the parameter set of the non-interacting part of the reference system. Within the VCA, the grand potential Ω of the original system per site is written by the following equation:

$$\Omega = \Omega_{\mathbf{t}'} - \frac{1}{N\pi} \int_0^\infty dx \sum_{\mathbf{K}} \ln |\det(1 - \hat{V}(\mathbf{K})) \hat{G}_{\mathbf{t}'}(ix)| + \frac{1}{2N} \sum_{\mathbf{K}} \text{tr} \hat{V}(\mathbf{K}), \quad (14)$$

where $\Omega_{\mathbf{t}'}$ is the exact ground potential of the reference system and $\hat{G}_{\mathbf{t}'}(z)$ is the Green's function of a decoupled cluster of the reference system. The matrix elements of $\hat{G}_{\mathbf{t}'}(z)$ are simply given by

$$(\hat{G}_{\mathbf{t}'}(z))_{a,a'} = \langle \psi_{\mathbf{t}'} | c_a(z + \mu' - H_{\mathbf{t}'} + E_{\mathbf{t}'})^{-1} c_{a'}^\dagger | \psi_{\mathbf{t}'} \rangle + \langle \psi_{\mathbf{t}'} | c_{a'}^\dagger(z + \mu' + H_{\mathbf{t}'} - E_{\mathbf{t}'})^{-1} c_a | \psi_{\mathbf{t}'} \rangle, \quad (15)$$

where a is the shorthand notation of $(\mathbf{r}_s, \alpha, \sigma)$ and \mathbf{r}_s is the site position in a decoupled cluster of the reference system. $H_{\mathbf{t}'}$ is the Hamiltonian in a decoupled cluster of the reference system with the ground state $|\psi_{\mathbf{t}'}\rangle$ and the ground state energy $E_{\mathbf{t}'}$. The chemical potential for the reference system is denoted by μ' . $\hat{G}_{\mathbf{t}'}(z)$ can be calculated using the continued fraction method. The matrix elements of $\hat{V}(\mathbf{K})$ is given by

$$(\hat{V}(\mathbf{K}))_{a,a'} = \frac{1}{N_c} \sum_{\mathbf{r}_c, \mathbf{r}'_c} (t_{A,A'} - t'_{A,A'}) e^{\mathbf{K} \cdot (\mathbf{r}_c - \mathbf{r}'_c)}, \quad (16)$$

where N_c is the number of clusters, A is the shorthand notation of $(\mathbf{r}_c + \mathbf{r}_s, \alpha, \sigma)$, \mathbf{r}_c is the position of the cluster, and $t_{A,A'}$ ($t'_{A,A'}$) indicates the coefficient of the term $c_{\mathbf{r},\alpha,\sigma}^\dagger c_{\mathbf{r}',\alpha',\sigma'}$ in the non-interacting part of the Hamiltonian for the original (reference) system, which includes the hopping parameter t_i ($i = 1-5$), the SOC λ , and the potential difference Δ . \mathbf{K} is the momentum for the superlattice of clusters defined by \mathbf{r}_c .

The choice of the parameter set \mathbf{t}' is arbitrary and, in principle, the best result should be obtained by searching for the optimized \mathbf{t}' which satisfies the stationary condition for Ω . However, computing directly Ω is impractical. For this reason, it is more convenient to start with an appropriate Weiss field. In previous section, we found that the low-energy magnetic excitations is similar to the ones of the effective Heisenberg model composed of the effective local Kramers doublet. Therefore, it is natural to introduce the following Weiss field for the reference system:

$$H' = h' \cos \phi' \sum_{\mathbf{r}} e^{i\mathbf{Q} \cdot \mathbf{r}} J_{\theta'}^x(\mathbf{r}) + h' \sin \phi' \sum_{\mathbf{r}} e^{i\mathbf{Q} \cdot \mathbf{r}} J_{\theta'}^z(\mathbf{r}), \quad (17)$$

with $\mathbf{Q} = (\pi, \pi)$. The variational parameters in \mathbf{t}' treated in this study are thus h' , θ' , and ϕ' , in addition to chemical potential μ' . For the optimization of multi-variables (h', θ', ϕ', μ'), we use the direction set method by optimizing one parameter at a time (with the remaining parameters fixed) iteratively until the full optimization is achieved for all parameters. The Brent's method is used for the optimization [19].

The most time consuming part in the VCA is the calculation for all the matrix elements of $\hat{G}(z)$. Because this calculation is independent, it is readily parallelized by using MPI without any trouble. We also parallelize the integral on x and summation over \mathbf{K} in (14). Figure 2 (a) shows the total elapsed time (t_e) versus the total number N_{core} of cores used to optimize two parameters, μ' and θ' , with a fixed system size. It is clearly seen in figure 2 (a) that t_e monotonically decrease with increasing N_{core} up to $N_{\text{core}} \sim 300$ without saturation. We define the following quantity r_s to evaluate the efficiency on the strong scaling of the parallelization:

$$r_s = \frac{t_e^* N_{\text{core}}}{t_e N_{\text{core}}^*}, \quad (18)$$

where N_{core}^* is a reference number of cores and t_e^* is the total elapsed time when N_{core}^* number of cores are used. Thus, $r_s = 1$ corresponds to 100% efficiency and usually r_s is less than one. As shown in fig. 2 (b), we find that our numerical scheme keeps $r_s > 0.8$ up to $N_{\text{core}} \sim 300$.

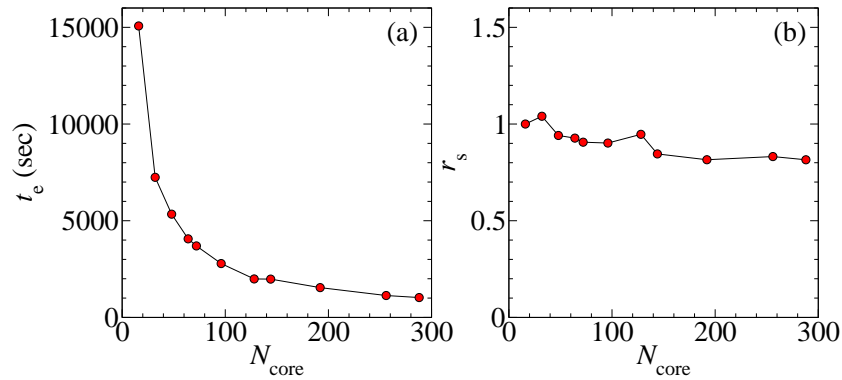


Figure 2. (a) Number of cores (N_{core}) dependence of the elapsed time t_e to optimize two parameters (μ', θ') for fixed h', ϕ' . The model parameters used here are given in the text, and a 4-site cluster is used. (b) N_{core} dependence of r_s [defined by (18)] for the parallel performance. The reference number of cores is $N_{\text{core}}^* = 8$.

4.2. Results

Figure 3 shows the variational parameter h' dependence of the ground state energy $E(h')$ obtained by the VCA using a 4-site cluster. The optimal h' is found to be $h' = 0.1892t_1$. A finite value of the optimal h' means that the system prefers to be symmetry broken. For all calculations, we find $\phi' = 0$, which indicates the effective Kramers doublet prefers to order antiferromagnetically with easy xy -plane anisotropy. This anisotropy is caused by the presence of the SOC and the Hund's coupling J . This finding is consistent with other theoretical results obtained by a strong-coupling theory [16], a 2-site exact diagonalization study [20], and a variational Monte Carlo study [11]. We also find in the VCA calculation that θ determined by minimizing the hole density $n_{\mathbf{r}\theta\sigma}$ is $\theta \sim 0.35\pi$, which is close to the value for the exact $J_{\text{eff}} = 1/2$ limit, i.e., $\theta = \arctan\sqrt{2} \sim 0.304\pi$.

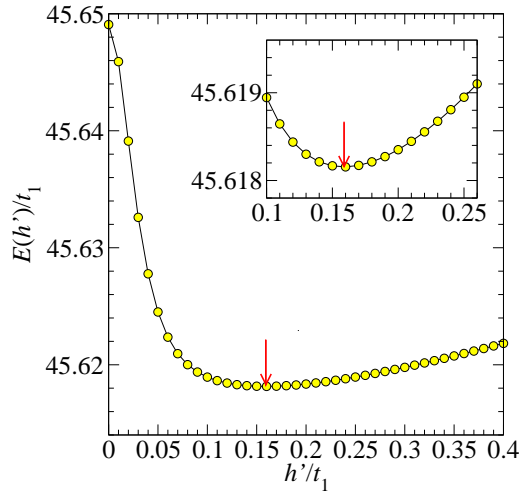


Figure 3. Variational parameter h' dependence of the energy $E(h')$ for the three-band Hubbard model [(1)] with a 4-site cluster. The other variational parameters (θ' , ψ' , μ') are optimized at each h' . The model parameters used are given in the text. The inset is an enlarged figure around the energy minima. Arrows indicate h' which gives the global minima of $E(h')$.

5. Conclusion

Using the numerically exact diagonalization technique, we have studied the magnetic excitations of the three-band Hubbard model with the strong SOC for Sr_2IrO_4 . We have found that the low-energy magnetic excitations are well described by those of the $J_{\text{eff}} = 1/2$ Kramers doublet, and that the lowest excitation dispersions can be reproduced by the antiferromagnetic Heisenberg model. We have estimated the effective exchange interaction as large as ~ 80 meV, which is in good agreement with recent experimental observations. We have also discussed the stability of the antiferromagnetically ordered ground state by using the VCA. We have found the ground state where the local Kramers doublet is in-plane antiferromagnetically ordered. These results strongly support the SOC induced $J_{\text{eff}} = 1/2$ Mott insulator for Sr_2IrO_4 .

Acknowledgments

The authors would like to thank H. Onishi and S. Fujiyama for fruitful discussions. The computation has been done using the RIKEN Cluster of Clusters (RICC) facility. This work has been supported by Grant-in-Aid for Scientific Research from MEXT Japan under the grant numbers 24740251 and 24740269.

References

- [1] Randall Jr J J, Katz L and Ward R 1957 *J. Am. Chem. Soc.* **79** 266
- [2] Okabe H, Isobe M, Takayama-Muromachi E, Koda A, Takeshita S, Hiraishi M, Miyazaki M, Kadono R, Miyake Y, and Akimitsu J 2011 *Phys. Rev. B* **83** 115118
- [3] Kim B J, Ohsumi H, Komesu T, Sakai S, Morita T, Takagi H and Arima T 2009 *Science* **323** 1329
- [4] Kim B J, Jin H, Moon S J, Kim J-Y, Park B-G, Leem C S, Yu J, Noh T W, Kim C, Oh S-J, Park J-H, Durairaj V, Cao G and Rotenberg E 2008 *Phys. Rev. Lett.* **101** 076402
- [5] Fujiyama S, Ohsumi H, Komesu T, Matsuno J, Kim B J, Takata M, Arima T and Takagi H 2012 *Phys. Rev. Lett.* **108** 247212
- [6] Kim J, Casa D, Upton M H, Gog T, Kim Y J, Mitchell J F, van Veenendaal M, Daghofer M, van den Brink J, Khaliullin G and Kim B J 2012 *Phys. Rev. Lett.* **108** 177003
- [7] For instance, Lyons K B, Fleury P A, Schneemeyer L F and Waszczak J V 1988 *Phys. Rev. Lett.* **60** 732
- [8] Potthoff M, Aichhorn M and Dahnen C 2003 *Phys. Rev. Lett.* **91** 206402
- [9] Potthoff M 2003 *Eur. Phys. J. B* **32** 429
- [10] Jin H, Jeong H, Ozaki T and Yu J 2009 *Phys. Rev. B* **80** 075112
- [11] Watanabe H, Shirakawa T and Yunoki S 2010 *Phys. Rev. Lett.* **105** 216410
- [12] Kanamori J 1963 *Prog. Theor. Phys.* **30** 275
- [13] Martins C, Aichhorn M, Vaugier L and Biermann S 2011 *Phys. Rev. Lett.* **107** 266404
- [14] Arita R, Kuneš J, Kozhevnikov A V, Eguiluz A G and Imada M 2012 *Phys. Rev. Lett.* **108** 086403

- [15] Dagotto E 1994 *Rev. Mod. Phys.* **66** 763
- [16] Jackeli G and Khaliullin G 2009 *Phys. Rev. Lett.* **102** 017205
- [17] Shirakawa T, Watanabe H, and Yunoki S 2011 *J. Phys. Soc. Jpn. Suppl.* **80** SB010
- [18] The low-lying peak in $M_\xi(\mathbf{q}, \omega)$ at $\mathbf{q} = 0$ corresponding to $J_\theta^\xi(\mathbf{q}, \omega)$ is too small to see in this scale, but there exists the corresponding peak in $M_\xi(\mathbf{q}, \omega)$ even at $\mathbf{q} = 0$.
- [19] Press W H, Teukolsky S A, Vetterling W T and Flannery B P 2007 *Numerical Recipes: The Art of Scientific Computing, Third Edition* (New York: Cambridge University Press) chapter 10 pp 497-515
- [20] Kim B H, Khaliullin G and Min B I 2012 *Phys. Rev. Lett.* **109** 167205